Comparison of Times of Synchronization of Chaotic Burke-Shaw Attractor with Active Control and Integer and Optimum Fractional-Order Pecaro Carroll Method

Ali Durdu (ali.durdu@asbu.edu.tr)
Social Sciences University of Ankara: Ankara Sosyal Bilimler Universitesi
Yılmaz Uyaroğlu
Sakarya University: Sakarya Universitesi

Research Article

Keywords: Active Control, Fractional-order, P-C method, Chaotic Systems, Synchronization

Posted Date: March 3rd, 2021

DOI: https://doi.org/10.21203/rs.3.rs-263593/v1

Comparison of Times of Synchronization of Chaotic Burke-Shaw Attractor with Active Control and Integer and Optimum Fractional-order Pecaro Carroll Method

Ali DURDU[1*], Yılmaz UYAROĞLU[2]

[1]Department of Management Information Systems, Faculty of Political Sciences*
Social Sciences University of Ankara, 06050 Altındağ, Ankara, Turkey
ali.durdu@asbu.edu.tr, https://orcid.org/0000-0002-5347-4491

[2]Department of Electrical & Electronics Engineering, Engineering Faculty
Sakarya University, 54187 Serdivan, Sakarya, Turkey
uyaroglu@sakarya.edu.tr, https://orcid.org/0000-0001-5897-6274

Abstract – Many studies have been introduced in the literature showing that two identical chaotic systems can be synchronized with different initial conditions. Secure data communication applications have also been made using synchronization methods. In the study, synchronization times of two popular synchronization methods are compared, which is an important issue for communication. Among the synchronization methods, active control, integer, and fractional-order Pecaro Carroll (P-C) method was used to synchronize the Burke-Shaw chaotic attractor. The experimental results showed that the P-C method with optimum fractional-order is synchronized in 2.35 times shorter time than the active control method. This shows that the P-C method using fractional-order creates less delay in synchronization and is more convenient to use in secure communication applications.

***Keywords**: Active Control, Fractional-order, P-C method, Chaotic Systems, Synchronization*

1. Introduction

Since chaotic systems are the most complex nonlinear steady-state behavior, they were considered unsuitable for synchronization. However, Pecora and Carroll showed that two identical chaotic systems with different initial conditions can synchronize and introduced the P-C method [1, 2]. After the P-C method was introduced, many synchronization methods were introduced. For the synchronization of two identical systems with different initial conditions, adaptive control [3], linear and nonlinear feedback control [4, 5], active control [6, 7], and passive control [8] have been proposed.

It has become a popular topic with the spread of synchronization methods and has been used in security applications. Using the synchronization of two identical chaotic systems, secure communication and information hiding studies have been introduced [9-11]. Liao and Lin [3] dealt with unknown system parameters and adaptive control and synchronization problems of Lorenz systems. Huang and et al. [4] synchronized two identical chaotic systems with a nonlinear control method based on Lyapunov stability theory. They tried their proposed method by applying it to two identical Lü systems and two different chaotic systems. Park [5] proposed a new nonlinear controller based on the Lyapunov stability theory by addressing the chaos synchronization problem of a chaotic system. The proposed controller ensures that the states of the controlled chaotic dependent system asymptotically synchronize the states of the host system. Yassen [6] presented chaos synchronization between two different chaotic systems using active control. Uçar et al. [7] investigated the synchronization of combined chaotic systems through active control. Synchronization is done in the slave-master program. The controller ensures that the states of the chaotic dependent system are exponentially synchronized with the state of the host system. Wang and Liu [8] investigated passive control synchronization. In their work, they designed a passive controller and performed synchronization of two identical combined chaotic systems with different initial conditions. Pehlivan et al. [9] used the P-C method to synchronize two identical chaotic systems with different initial conditions and implement chaotic encrypted information signal transfer. Akgül et al. [10] performed a data hiding method with a three-dimensional chaotic system without an equilibrium point. In the study, a new data hiding method based on chaos that hides an image of a different color to color images is proposed. Through the proposed method, the data is hidden in bit spaces inside the image with the help of a chaotic random number generator (RNG). Cheng and cheng [11] tried to develop a robust synchronization scheme for two different chaotic systems exposed to limited noise. The synchronization controller they proposed is embedded in a secure communication scheme that is not only resistant to channel noise but can also include the noise as part of the encryption key, thus increasing the key security. Ojo et al. [12] examined synchronization methods in their study and presented their advantages and disadvantages compared to each other. Khan and Chaudhary [13] studied the hybrid projective combination synchronization scheme between identical chaotic generalized Lotka-Volterra three types of biological systems using active control design. Kocamaz and Uyaroğlu [14] presented the chaos synchronization and anti-synchronization of the Single Machine Infinite Bus (SMIB) power system to the Duffing oscillator using the active control method. Matouk [15] synchronized the autonomous Duffing-Van der Pol system modified with integer-order and fractional-order P-C method. Also, the synchronization between two different fractional-order chaotic systems is studied and the fractional-order Lu system is controlled as the fractional-ordered Chen system. In the work of Zhu et al. [16] based on the stability theorem of linear fractional systems, a necessary condition is given to control the chaos synchronization of disproportionate ordered fractional systems. Wang et al. [17] proposed the synchronization of a fractional time delay financial system using a new type-2 fuzzy active control method. Sahin et al. [18] proposed a new four-dimensional (4D) chaotic system comprising an active flux controlled memristor characterized by a uniform continuous cubic nonlinearity. Yu et al. [19] proposed a new 5D hyperchaotic four-bladed memristive system (HFWMS) by developing a quadratic nonlinear flux-controlled memristor to the 4-dimensional hyperchaotic system as the feedback term. Al-khedhairi [20] recently introduced a new financial model based on a non-smooth fractional-order Caputo-Fabrizio derivative. Chaos synchronization between the two master / slave fractional financial models has been obtained based on the adaptive control theory. Carbajal-Gomez et al. [21] proposed a current mode segmented linear (PWL) function based on CMOS cells that allow programmable generation of 2-7 shift chaotic attractors. Also, they showed that it is suitable for secure communication by providing synchronization of 2-7 slide towers in a master-slave topology with generalized Hamilton forms and observer approach. Bhardwaj and Das [22] investigated the synchronization problem of two-three types of models with the Beddington-DeAngelis type functional response using the master-dependent scheme. Based on the selected intrinsic growth parameters that characterize the complex dynamics of the master and dependent system, active controller functions that cause general asymptotic stability of synchronization errors for cases I and II, respectively, are obtained. Emiroğlu and Uyaroğlu [23] have synchronized Burke-Shaw's chaotic attraction with active control.

The most important issue in security applications created using the synchronization method is the synchronization time of the two chaotic systems. The shorter the synchronization time, the better the communication quality in secure communication applications. This is due to the short delay created by the synchronization times. When the delay in communication is short, the communication quality increases.

In this study, the Burke-Shaw chaotic attractor is introduced and the Burke-Shaw chaotic system, which has two different starting points, has been synchronized with both the active control method and the P-C method with integer and optimum fractional-order value. Each synchronization method is modeled and implemented in Matlab ™ environment. It is shown with error graphs that two systems are synchronized in each synchronization system. In the study, synchronization times of synchronization methods were compared. The experimental results showed that the optimum fractional-order value P-C method synchronizes in 2.3 (time unit) less than the active control method and 4.3 (time unit) compared to the integer-order P-C method. This shows that the P-C method using fractional-order creates less delay in synchronization and is more convenient to use in secure communication applications. In the second part of this study, Matlab-Simulink modeling is given by introducing the Burke-Shaw chaotic attractor. In the third chapter, synchronization with the active control method is explained and synchronization graphics are given. In the fourth chapter, synchronization with fractional-order P-C method is explained, synchronization graphics are given and synchronization times of all synchronization methods are compared. Results are given in the last section.

2. Burke-Shaw Chaotic Attractor

Burke-Shaw chaotic attractor was created by Bill Burke and Robert Shaw derived from the Lorenz chaotic equation [24]. The equation set for the Burke-Shaw chaotic attractor is given in (1). In (1) has x, y, and z state variables and s and V system parameters. As seen in the equation in (1), it is seen that the Burke-Shaw chaotic attractor is a 3rd-degree chaotic system. The Burke-Shaw chaotic attractor has been implemented in the Matlab-Simulink environment and the Matlab-Simulink model is given in Fig. 1. Where s and V are real constants. For a specific value of the parameters such as $s=10$, $V=13$ with the initial value (0.1, 0.1, 0.1), which makes the Burke-Shaw attractor chaotic. The x-y-z time series and the phase portraits of the state variables are given in Figs. 2 and 3.

Burke-Shaw chaotic attractor nonlinear equation system is given in (1).

$$\begin{aligned} \dot{x} &= -s(x+y) \\ \dot{y} &= -y - sxz \\ \dot{z} &= sxy + V \end{aligned} \tag{1}$$

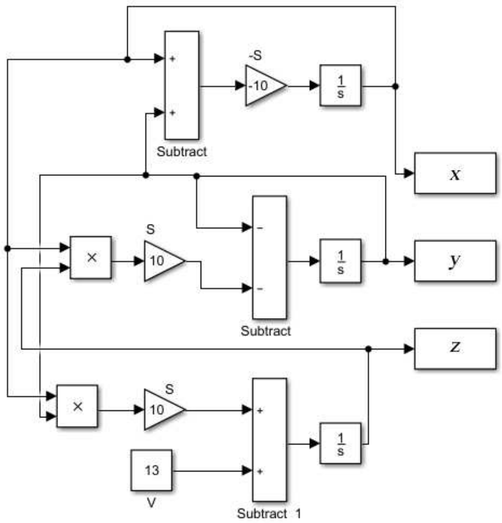

Fig. 1 Matlab-Simulink model of Burke-Shaw chaotic attractor.

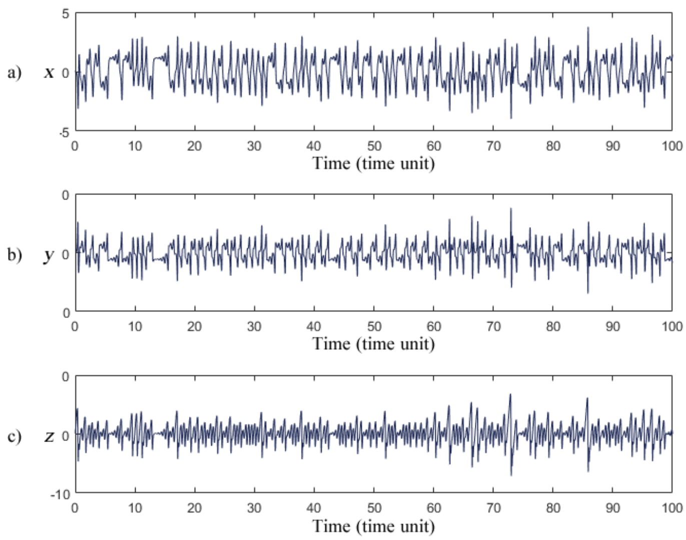

Fig. 2 *x, y,* and *z* time series for Burke-Shaw chaotic attractor: a) *x* b) *y* c) *z*.

Lyapunov exponentials of the Burke-Shaw chaotic attractor are calculated with (2) and the Lyapunov graph is plotted in Matlab environment and is given in Fig. 4.

$$\lambda = \frac{1}{t_N - t_0} \sum_{k=1}^{N} \log_2 \frac{d\left(t_k\right)}{d\left(t_{k-1}\right)} \tag{2}$$

As seen in Fig. 4, Lyapunov exponentials are calculated as $\lambda_1 = 2.24 < 0, \lambda_2 = 0, \lambda_3 = -13.24 < 0$. Burke-Shaw shows that the chaotic attractor exhibits chaotic behavior, as λ_1 is positive, λ_2 is zero, and λ_3 is negative according to Lyapunov exponential values.

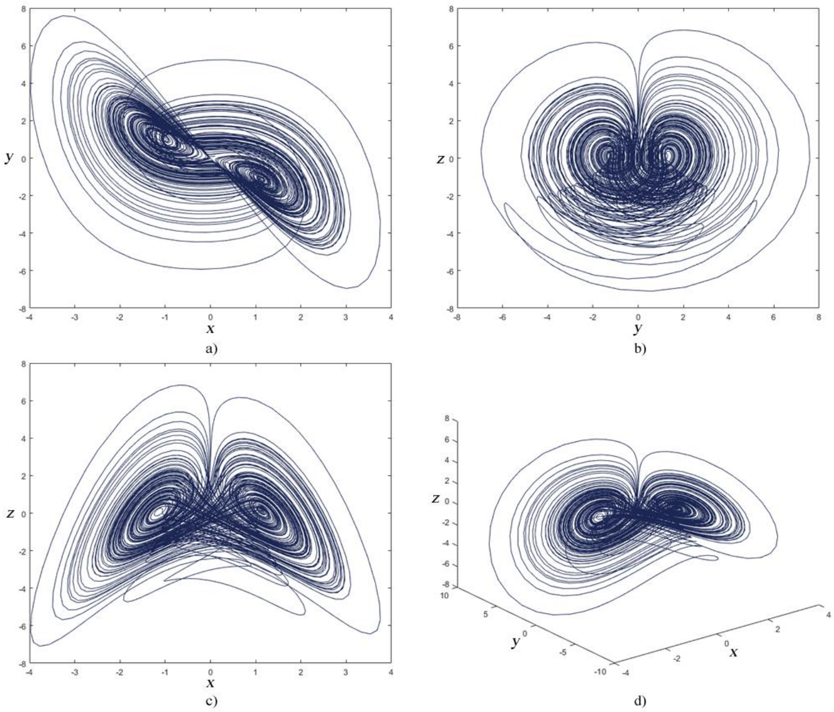

Fig. 3 Phase portraits of a Burke-Shaw chaotic attractor*:* a*) x-y,* b) *y-z,* c) *x-z,* d) *x-y-z*.

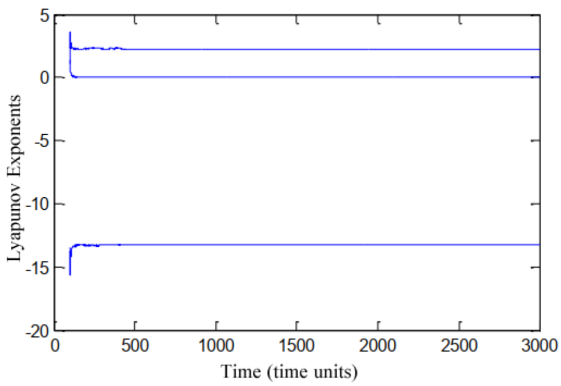

Fig. 4 Lyapunov exponents of a Burke-Shaw chaotic attractor.

3. Synchronization with Active Control

Two identical Burke-Shaw chaotic attractors with different initial conditions are synchronized by the active control method. In (3), the driver system equation of the active control method is given. The response system that will respond to the driver system is given in (4).

$$
\begin{aligned}
\dot{x}_1 &= -s\left(x_1 + y_1\right) \\
\dot{y}_1 &= -y_1 - s x_1 z_1 \\
\dot{z}_1 &= s x_1 y_1 + V
\end{aligned}
\tag{3}
$$

In (4), *u1(t)*, *u2(t),* and *u3(t)* are control functions that provide synchronization with active control between the driver and the responder system and are given in (5). The *v1(t)*, *v2(t)* and *v3(t)* given in (5) are control inputs.

$$\begin{aligned} \dot{x}_2 &= -s\left(x_2 + y_2\right) + u_1(t) \\ \dot{y}_2 &= -y_2 - s x_2 Z_2 + u_2(t) \\ \dot{z}_2 &= s x_2 y_2 + V + u_3(t) \end{aligned} \tag{4}$$

$$\begin{aligned} u_1(t) &= v_1(t) \\ u_2(t) &= s x_2 z_2 - s x_1 z_1 + v_2(t) \\ u_3(t) &= s x_1 y_1 - s x_2 y_2 + v_3(t) \end{aligned} \tag{5}$$

Driver and responder in (3) and (4) are defined as the error between the two systems. To find the synchronization errors, the driver system is removed from the answering system, and the error dynamic system in (6) is obtained.

$$\begin{aligned} \dot{e}_1 &= -s\left(e_1 + e_2\right) + u_1(t) \\ \dot{e}_2 &= -e_2 - s x_2 z_2 + s x_1 z_1 + u_2(t) \\ \dot{e}_3 &= s x_2 y_2 - s x_1 y_1 + u_3(t) \end{aligned} \tag{6}$$

If the control functions in (5) are replaced by the error in (6) in the dynamic system, the equations in (7) are obtained.

$$\begin{aligned} \dot{e}_1 &= -s\left(e_1 + e_2\right) + v_1(t) \\ \dot{e}_2 &= -e_2 + v_2(t) \\ \dot{e}_3 &= v_3(t) \end{aligned} \tag{7}$$

In active control, control inputs *v1(t)*, *v2(t),* and *v3(t)* control the error system in (6), converting the error to zero, which indicates that synchronization has been achieved. The control inputs *v1(t)*, *v2(t),* and *v3(t)* are selected as shown in the matrix in (8).

$$\begin{bmatrix} v_1(t) \\ v_2(t) \\ v_3(t) \end{bmatrix} = B \begin{bmatrix} e_1 \\ e_2 \\ e_3 \end{bmatrix}, \quad B = \begin{bmatrix} s-1 & s & 0 \\ 0 & 0 & 0 \\ 0 & 0 & -1 \end{bmatrix} \tag{8}$$

In (8), the *B* matrix is a constant matrix, and all eigenvalues must be negative for the error system in (7) to be asymptotically stable. All eigenvalues of matrix *B* given in (8) were chosen to be negative. In the last case, the error dynamic system is given in (9).

$$\begin{aligned} \dot{e}_1 &= -e_1 \\ \dot{e}_2 &= -e_2 \\ \dot{e}_3 &= -e_3 \end{aligned} \tag{9}$$

The Lyapunov function suitable for the error cases *e1(t)*, *e2(t),* and *e3(t)* in the dynamic system of the error obtained in (9) is given in (10). When the derivative of the Lyapunov function in (10) is taken, the equation in (11) is obtained.

$$V\left(e_1, e_2, e_3\right) = \frac{1}{2}\left(e_1^2 + e_2^2 + e_3^2\right) \tag{10}$$

$$\frac{dV}{dt} = -\left(e_1^2 + e_2^2 + e_3^2\right) \tag{11}$$

Since the V in (11) is negative, the driver (3) and the responder (4) systems are asymptotically stable, which is proof that the two systems are synchronized. The systems were run by taking different initial conditions $\left[x_1(0), y_1(0), z_1(0)\right]^T = [0.6, 0, 0]^T$ and $\left[x_2(0), y_2(0), z_2(0)\right]^T = [4, 2, -3]^T$ respectively for driver and receiver systems implemented in Matlab environment. Fig. 5 shows the *x-y-z* time series of the driver and responder systems before active synchronization and the synchronization error signals between the two systems. When the *x-y-z* time series in Fig. 5.a, b and c are examined, it is seen that the two systems are not synchronized and have different values at the same time. When the error signals showing the difference of x-y-z state variables between the driver and receiver systems in Fig. 5.d are examined, it shows that the driver and receiver systems are not synchronized, all state variables generate values throughout the entire time series and do not converge to zero. In Fig. 6, after active synchronization, the *x-y-z* time series of the driver and responder systems and the synchronization error signals between the two systems are given. When the x-y-z time series in Fig. 6.a, b and c are examined, it is seen that the two systems are synchronized and all state variables of the two systems are at the same values after 4 (time unit) time. When the error signals showing the difference of *x-y-z* state variables between the driver and receiver systems in Fig. 6.d are examined, the convergence of all state variables to zero after 4 (time unit) time shows that the driver and receiver systems are synchronized.

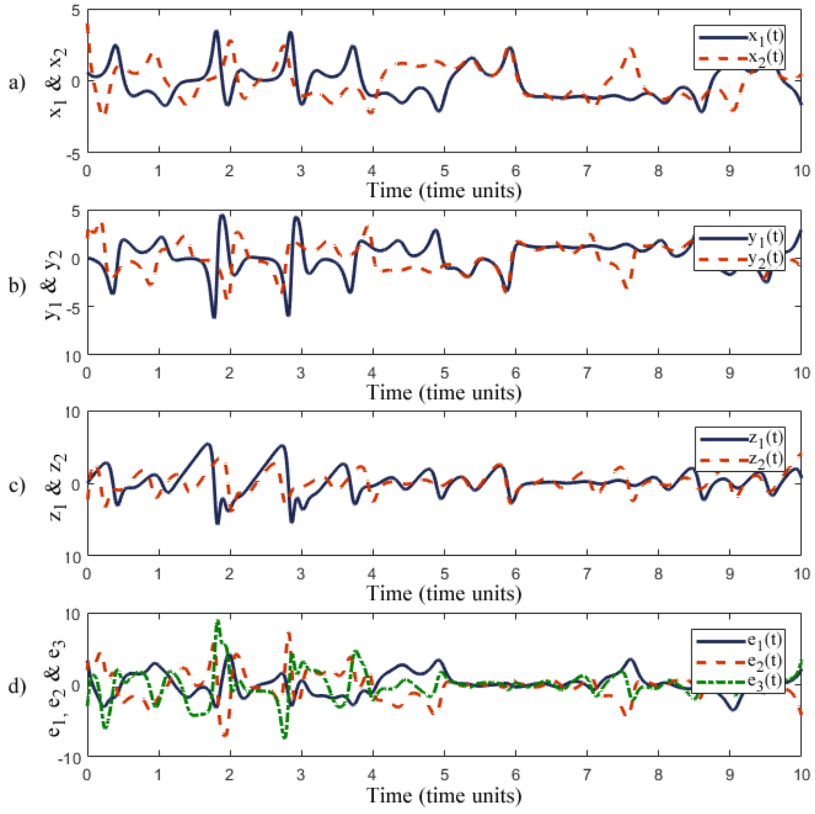

Fig. 5 Before active control synchronization (a) driving and response signal (x_1, x_2), (b) y_1 and y_2 , (c) z_1 and z_2, (d) errors ($e_1 = x_1\text{-}x_2$, $e_2 = y_1\text{-}y_2$, $e_3 = z_1\text{-}z_2$)

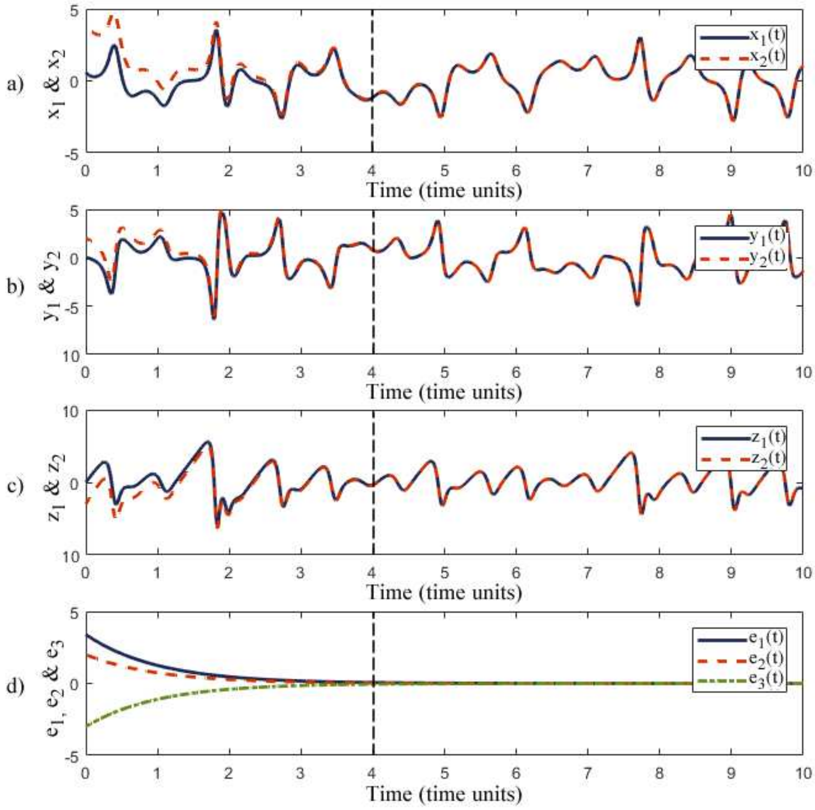

Fig. 6 Post active control synchronization (a) driving and response signal (x_1, x_2), (b) y_1 and y_2 , (c) z_1 and z_2, (d) errors ($e_1 = x_1$-x_2, $e_2 = y_1$-y_2, $e_3 = z_1$-z_2)

4. Synchronization with Fractional-order P-C Method

Pecora and Carroll arbitrarily divide an original chaotic system they discussed in their work into two separate parts and named them driver and responder subsystems. They showed that by creating the same responsive subsystem in the receiver module, chaotic synchronization can be achieved if this subsystem is driven with the driver part of the original system. In other words, they have shown both theoretically and experimentally that the chaotic signal generated in the receiver module will converge to the chaotic signal coming from the original system [1]. Fig. 4 shows the operating system of the P-C synchronization method. As seen in Fig. 4, the *x*, *y,* and *z* state variables directly stimulate the responder subsystem. The responder system is divided into two subsystems. In the responder system, variable *x* for the first subsystem is warned from the driver system, while variable *y* for the second subsystem is warned from the first subsystem. Fractional-order applied Burke-Shaw chaotic attractor is synchronized with the P-C method.

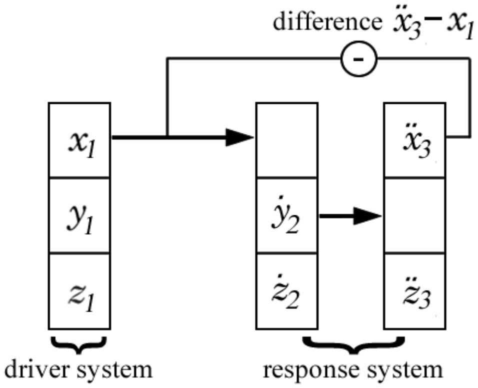

Fig. 7 The block diagram of P-C synchronization [1].

In the P-C method, the equation of the fractional-order Burke-Shaw chaotic attractor driver system given in Fig. 7 is given in (12).

$$
\begin{aligned}
\frac{d^q x_1}{dt^q} &= -\mathrm{s}\left(\mathrm{x}_1 + \mathrm{y}_1\right) \\
\frac{d^q y_1}{dt^q} &= -\mathrm{y}_1 - \mathrm{s}\mathrm{x}_1\mathrm{z}_1 \\
\frac{d^q z_1}{dt^q} &= \mathrm{s}\mathrm{x}_1\mathrm{y}_1 + \mathrm{V}
\end{aligned}
\tag{12}
$$

The first order ($\dot{y}_2$ and $\dot{z}_2$) stable first sub responder system of the P-C method is given in (13).

$$
\begin{aligned}
\frac{d^q \dot{y}_2}{dt^q} &= -\dot{y}_2 - \mathrm{s}\mathrm{x}_1\dot{z}_2 \\
\frac{d^q \dot{z}_2}{dt^q} &= \mathrm{s}\mathrm{x}_1\dot{y}_2 + \mathrm{V}
\end{aligned}
\tag{13}
$$

Likewise, a second-order ($\ddot{x}_3$ and $\ddot{z}_3$) stable second sub responder system is given in (14).

$$
\begin{aligned}
\frac{d^q \ddot{x}_3}{dt^q} &= -\mathrm{s}\left(\ddot{x}_3 + \dot{y}_2\right) \\
\frac{d^q \ddot{z}_3}{dt^q} &= \mathrm{s}\ddot{x}_3\dot{y}_2 + \mathrm{V}
\end{aligned}
\tag{14}
$$

In the P-C synchronization realized with integer-order in the Matlab environment, the driver (12) and receiver systems (13, 14) were taken with the same initial conditions as the active control, and the systems were operated. In Fig. 8, while all conditions are the same, synchronization error signals between the two systems with the *x*-*y*-*z* time series of the driver and responder systems after P-C synchronization with integer-order are given. When the *x*-*y*-*z* time series in

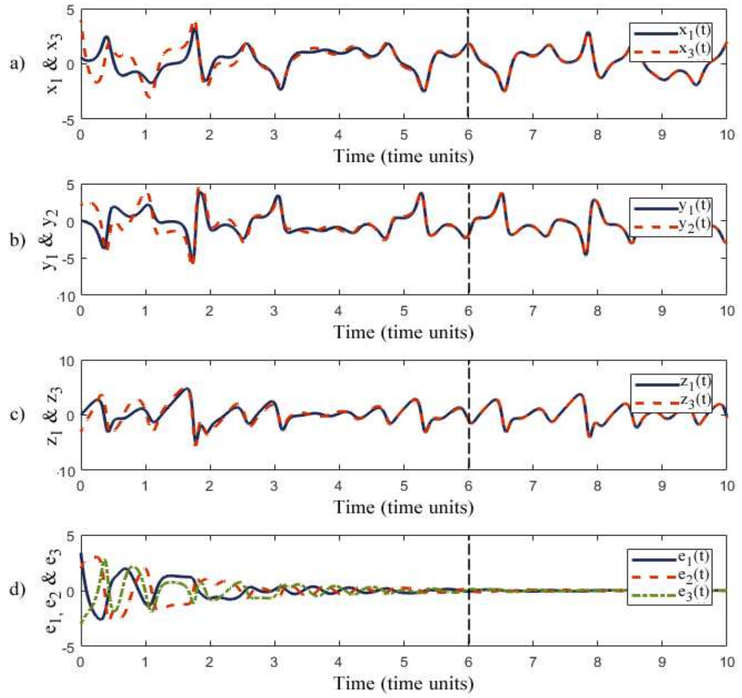

Fig. 8 Post P-C synchronization with integer-order (a) driving and response signal (x_1, x_3), (b) y_1 and y_2 , (c) z_1 and z_3, (d) errors ($e_1 = x_1 - x_3$, $e_2 = y_1 - y_2$, $e_3 = z_1 - z_3$)

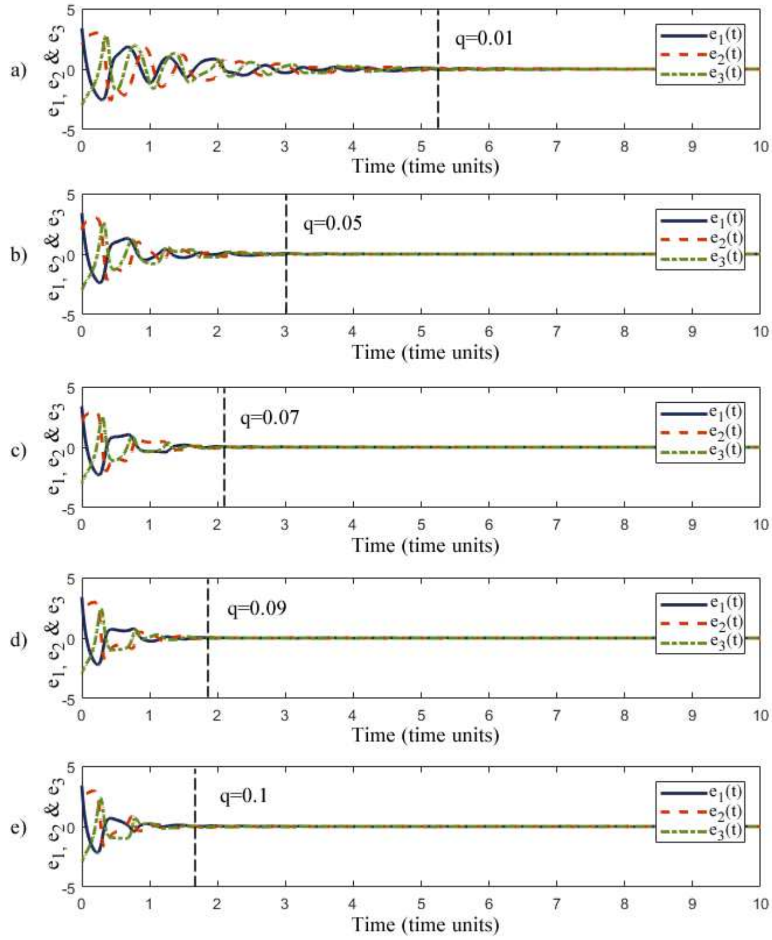

Fig. 9 Post P-C synchronization with fractional-order errors for various fractional-order *q* values

Fig. 8.a, b and c are examined, it is seen that the two systems are synchronized and all state variables of the two systems are at the same values after 6 (time unit) time. When the error signals showing the difference of *x-y-z* state variables between the driver and receiver systems in Fig. 8.d are examined, the convergence of all state variables to zero after 6 (time unit) time shows that the driver and receiver systems are synchronized.

In the P-C synchronization implemented using fractional-order in Matlab environment, the driver (12) and receiver systems (13, 14) were re-operated under the same initial conditions as the active control. The Burke-shaw fractional order chaotic system was modelled with nid function, one of Ninteger fractional control toolbox for Matlab tools [25]. The Burke-Shaw chaotic P-C synchronization system was tested with different fractional-order values in the range of $0<q<1$ and the optimum fractional-order value was tried to be found. Here, the condition that ensures optimum fractional-order is the condition of the chaotic system to be synchronized as soon as possible. Fig. 9 shows the synchronization error graphs of the chaotic system in P-C synchronization, which is implemented using the shortest-time optimum five fractional-order values from all fractional-order values. Accordingly, the results for the five values q= [0.01, 0.05, 0.07, 0.09 and 0.1] are given in Fig. 9, respectively. When Fig. 9 is examined, when q = 0.01, the system synchronizes in 5.2 (time unit) time, while at q = 0.1, the system synchronizes in 1.7 (time unit).

Fig. 10 shows the graph showing P-C synchronization times with different *q* values of the fractional-order Burke-Shaw chaotic system. The effect of the change in *q* value in Fig. 9 on the synchronization time can be seen more clearly on the graph in Fig. 10. When Fig. 10 is examined, it clearly shows that the increase in *q* value leads to a decrease in synchronization time. Accordingly, the optimum fractional-order value was determined as 0.1 because the system synchronized with a 1.7 (time unit) value in the shortest time.

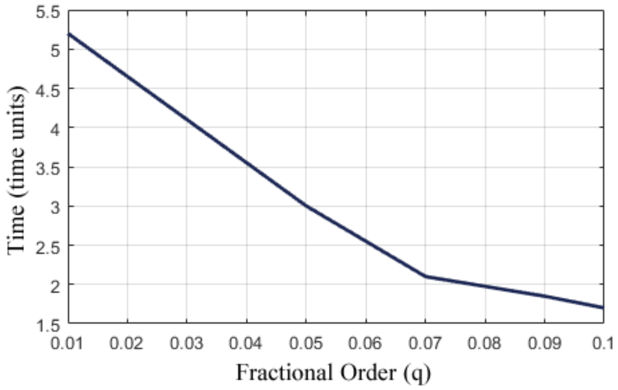

Fig. 10 Post P-C synchronization with fractional-order times for various fractional-order *q* values

Table 1 shows the data showing the behavior of the fractional-order Burke-shaw chaotic attractor given in (12) at different fractional-order values. According to Table 1, the fractional-order Burke-shaw chaotic attractor shows its chaotic features at the intervals of $0.01 \leq q \leq 0.1$ and $0.8 \leq q \leq 0.99$, while it emerges from its chaotic feature in the range of $0.2 \leq q \leq 0.7$. Accordingly, the fractional-order value is in the range of $0.2 \leq q \leq 0.7$, the system emerges from chaotic behavior and this situation affects P-C synchronization and does not provide synchronization. When the already sensitive structure of the Burke-Shaw chaotic system works with fractal values at high values, it causes the system to exit chaotic behavior.

Table 1 Burke-Shaw chaotic attractor behavior for various fractional-order *q* values

Fractional-order (q)	Behavior
$0.01 \leq q \leq 0.1$	Chaotic
$0.2 \leq q \leq 0.7$	Non-chaotic
$0.8 \leq q \leq 0.99$	Chaotic

In Table 2, the synchronization times of the Burke-Shaw chaotic attractor and active control, P-C method, and fractional-order P-C method methods are compared. Accordingly, the active control method obtains 4 (time units) as the synchronization time. Integer-order P-C method obtained a value of 6 (time unit) during the synchronization period. When fractional-order is used, it is synchronized at 5.2 (time unit) when q = 0.01, 3 (time unit) when q = 0.05, 2.1 (time unit) when q = 0.07, 1.85 (time unit) when q = 0.09, and at 1.7 (time unit) when q=0.1. According to the results, the P-C method, which uses the optimum fractional-order value, achieves very successful results compared to the active control method.

Table 2 Comparison of synchronization times of active control, integer and fractional-order p-c synchronization methods

Method		Time (time unit)
Active Control		4
P-C with integer-order		6
P-C with fractional-order (q)	0.01	5.2
	0.05	3
	0.07	2.1
	0.09	1.85
	0.1	1.7

When all the results of the study are evaluated, the P-C method, which uses the optimum fractional-order value, synchronizes in a shorter time of 2.3 (time unit) compared to the active control. This shows that the optimum fractional-order value significantly shortens the synchronization time in the P-C method. When the fractional-order value is q = 0.01, it synchronizes at the value of 5.2 (time unit), while the synchronization time decreases even more as the fractional-order value increases up to the value of q = 0.1. While the fractional-order value is q = 0.01, it lags in the synchronization period of the active control method with the value of 5.2 (time unit), while at the value of q = 0.05, it has started to exceed the synchronization time of the active control method with a value of 3 (time unit).

When the synchronization errors of the active control method in Fig. 6.d were examined, it was seen that the error values of the *x-y-z* state variables remained constant at positive or negative values and converged to zero with regular decreases. In the P-C method in Fig 8.d, it is seen that the error values of the *x-y-z* state variables change in positive and negative values and converge to zero with a fluctuating decrease. This difference in the error graphs is due to the differences in the working structures of the methods. At q = 0.1, where the fractional-order value is low, the main reason for the system to synchronize in a shorter time is that the Burke-Shaw system is already sensitive and even at a low fractional value, the system has synchronized in a short time.

The most important issue in security applications created using the synchronization method is the synchronization time of the two chaotic systems. The shorter the synchronization time, the better the communication quality in secure communication applications. This is due to the short delay created by the synchronization times. When the delay in communication is short, the communication quality increases. The P-C method using the optimum fractional-order value significantly reduces the synchronization time. This is an indication that it is more suitable for use in secure communication applications.

5. Conclusion

In this study, synchronization times of Burke-Shaw chaotic attractor and active control, integer, and fractional-order P-C methods are compared. The experimental results showed that the P-C method with optimum fractional-order is synchronized in 2.35 times shorter time than the active control method. P-C method synchronization times with different fractional-order values were compared and optimum fractional-order was found to be 0.1. It was seen that the optimum fractional-order value and the synchronization time were 1.7 (time unit). Since the fractional valued P-C method is synchronized in a shorter time, the information signal can be transferred to the target immediately with a short delay in communication. The low delay indicates that the optimally valued fractional-order P-C synchronization method will be more suitable in secure communication applications, since the transmitted signals and received signals are the same and the error rates are always around zero.

References

[1] Pecora, L.M., Carroll, T.L.: Synchronization in chaotic systems. Phys. Rev. Lett. 64, 8, 821 (1990).

[2] Pecora, L. M., Carroll, T. L.: Driving systems with chaotic signals. Physical Review A.44, 4, 2374–83 (1991).

[3] Liao, T.L., Lin, S.H.: Adaptive control and synchronization of Lorenz systems. J. Franklin Inst. 336, 925–937 (1999).

[4] Huang, L., Feng, R., Wang, M.: Synchronization of chaotic systems via nonlinear control. Phys. Lett. Sect. A. 320, 4, 271-275 (2004).

[5] Park, J.H.: Chaos synchronization of a chaotic system via nonlinear control. Chaos, Solitons & Fractals. 25, 3, 579-584 (2005).

[6] Yassen, M.T.: Chaos synchronization between two different chaotic systems using active control. Chaos, Solitons and Fractals. 23,1, 131-140 (2003).

[7] Uçar, A., Lonngren, K.E., Bai, E.W.: Synchronization of the unified chaotic systems via active control. Chaos, Solitons & Fractals. 27, 5 1292-1297 (2006).

[8] Faqiang, W., Chongxin, L.: Synchronization of unified chaotic system based on passive control, Physica D. 225, 55–60 (2007).

[9] Pehlivan, İ., Uyaroğlu, Y., Yalçın, M.A., Ferikoğlu, A.: Sprott_94_A Kaotik Sisteminin Senkronizasyonu ve Bilgi Gizlemede Kullanılması. Uluslararası Katılımlı Bilgi güvenliği ve Kriptoloji Konferansı. Ankara, Türkiye, 230-237 (2007).

[10] Akgül, A., Moroz, I., Durdu, A.: A novel data hiding method by using a chaotic system without equilibrium points. Modern Physics Letters B. 33, 29, 1950357 (2019).
[11] Cheng, C., Cheng, C.: Robust synchronization of chaotic systems subject to noise and its application to secure communication. 2012 Fourth International Conference on Computational Intelligence, Communication Systems and Networks, Phuket, Thailand, 206-210 (2012).
[12] Ojo, K. S., Njah, A. N., & Ogunjo, S. T.: Comparison of backstepping and modified active control in projective synchronization of chaos in an extended Bonhöffer-van der Pol oscillator. Pramana - Journal of Physics. 80, 825–835 (2013).
[13] Khan, T., Chaudhary, H.: Controlling and Synchronizing Combined Effect of Chaos Generated in Generalized Lotka-Volterra Three Species Biological Model using Active Control Design. Appl. Appl. Math. 15, 2, 1135–1148 (2020).
[14] Kocamaz, U. E., & Uyaroglu, Y.: Non-Identical Synchronization, Anti-Synchronization and Control of Single-Machine Infinite-Bus Power System via Active Control. Information Technology and Control. 43, 2, 166–174 (2014).
[15] Matouk, A. E.: Synchronization in Integer and Fractional-order Chaotic Systems. In Chaos Synchronization and Cryptography for Secure Communications: Applications For Encryption. 127–151 (2011).
[16] Zhu, H., Zhou, S., He, Z: Chaos synchronization of the fractional-order Chen's system. Chaos, Solitons & Fractals, 41, 5, 2733–2740 (2009).
[17] Wang, S., Bekiros, S., Yousefpour, A., He, S., Castillo, O., Jahanshahi, H.: Synchronization of fractional time -delayed financial system using a novel type-2 fuzzy active control method. Chaos, Solitons & Fractals, 136 (2020).
[18] Sahin, M. E., Taskiran, Z. G. C., Guler, H., Hamamci, S. E.: Application and Modeling of a Novel 4D Memristive Chaotic System for Communication Systems. Cırcuits Systems and Signal Processing, 39, 7, 3320–3349 (2020).
[19] Yu, F., Liu, L., He, B., Huang, Y., Shi, C., Cai, S., Song, Y., Du, S., Wan, Q.: Analysis and FPGA Realization of a Novel 5D Hyperchaotic Four-Wing Memristive System, Active Control Synchronization, and Secure Communication Application. Complexity (2019).
[20] Al-khedhairi, A.: Dynamical analysis and chaos synchronization of a fractional-order novel financial model based on Caputo-Fabrizio derivative. European Physical Journal Plus 134, 10 (2019).
[21] Hugo Carbajal-Gomez, V., Tlelo-Cuautle, E., Sanchez-Lopez, C., Vidal Fernandez-Fernandez, F.: PVT-Robust CMOS Programmable Chaotic Oscillator: Synchronization of Two 7-Scroll Attractors, Electronics, 7, 10 (2018).
[22] Bhardwaj, R., Das, S.: Synchronization of two three-species food chain system with Beddington-DeAngelis functional response using active controllers based on the Lyapunov function. Italian Journal of Pure and Applied Mathematics. 44, 57–77 (2020).
[23] Emiroğlu, S., Uyaroğlu, Y.: Synchronization of Chaotic Burke-Shaw Attractor Via Active Control. Engineering Sciences. 6, 325–331 (2011).
[24] Shaw, R.: Strange Attractors, Chaotic Behavior, and Information Flow. Zeitschrift fur Naturforsch. - Sect. A J. Phys. Sci. (1981).
[25] Duarte V. Ninteger v. 2.3 Fractional control toolbox for MatLab. (2005).

Declarations

Funding

There is no funding available.

Conflicts of interest/Competing interests

There are no conflicts of interest regarding the publication of this paper.

Availability of data and material

No data were used to support this study.

Code availability

The codes used in this article were written by the authors and can be used on demand.

Authors' contributions

Ali DURDU: Corresponding author and undertakes more than 80% of the article.
Yılmaz Uyaroğlu: He has serious efforts in consultant position and publication.

Figures

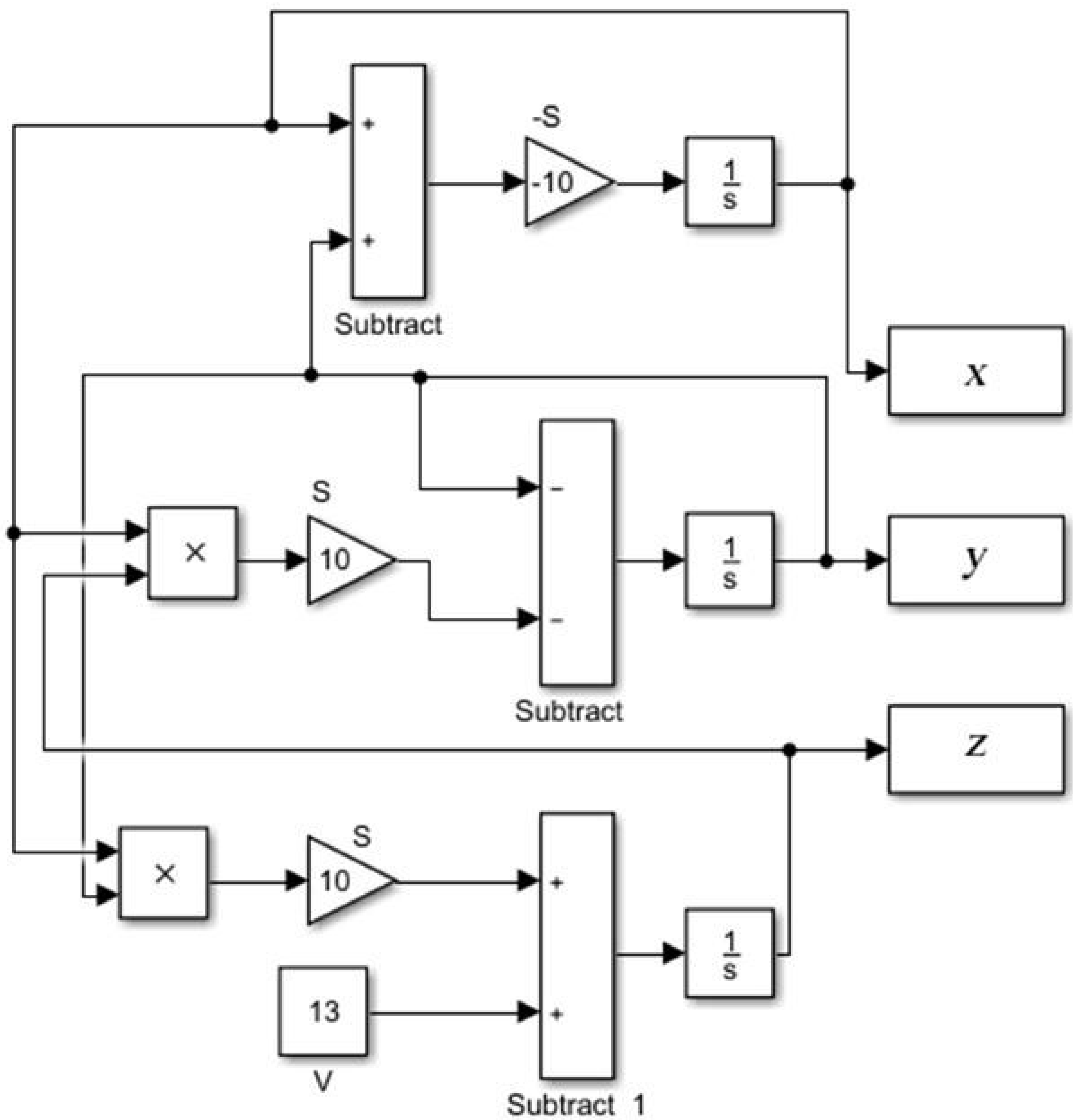

Figure 1

Matlab-Simulink model of Burke-Shaw chaotic attractor.

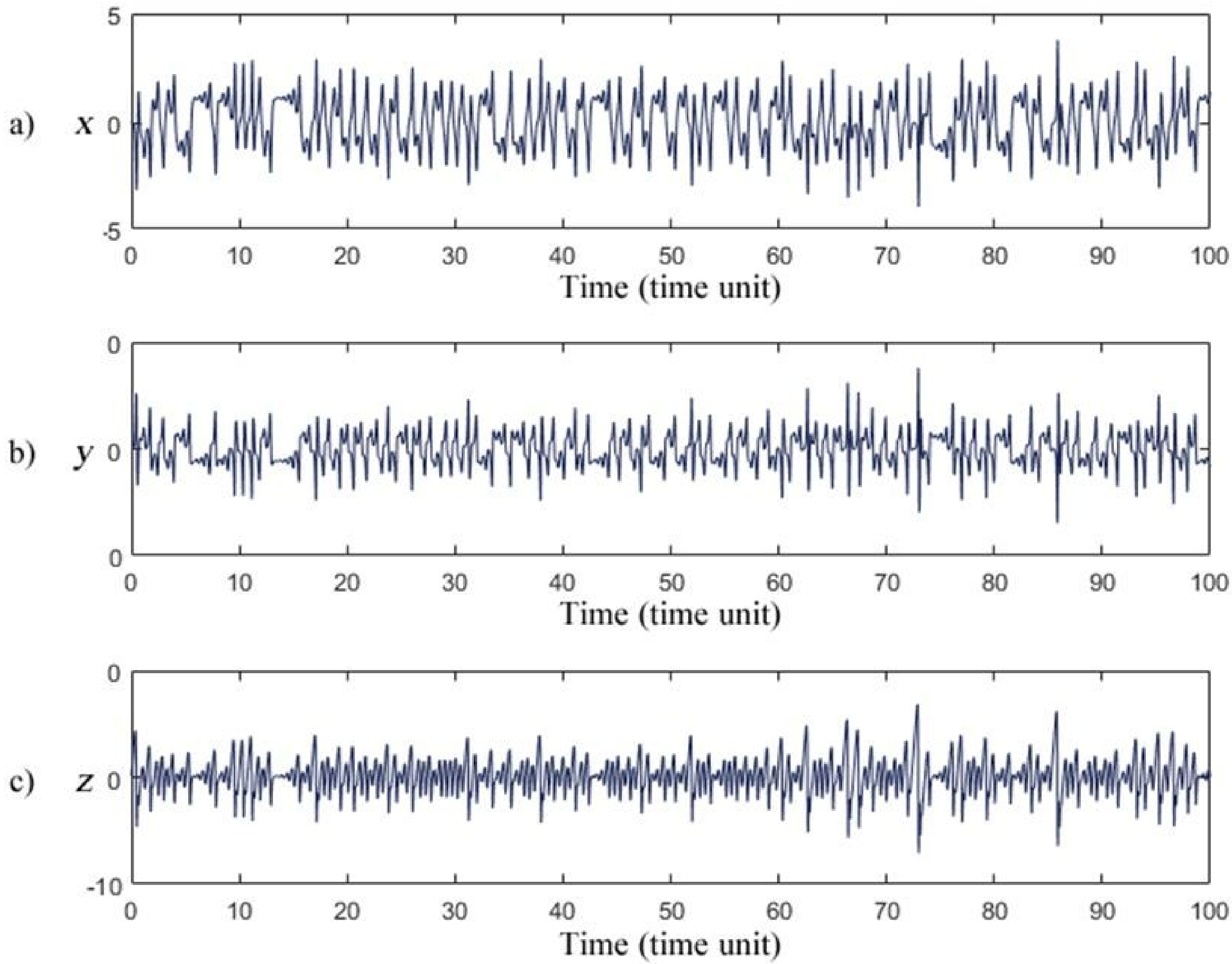

Figure 2

x, y, and z time series for Burke-Shaw chaotic attractor: a) x b) y c) z.

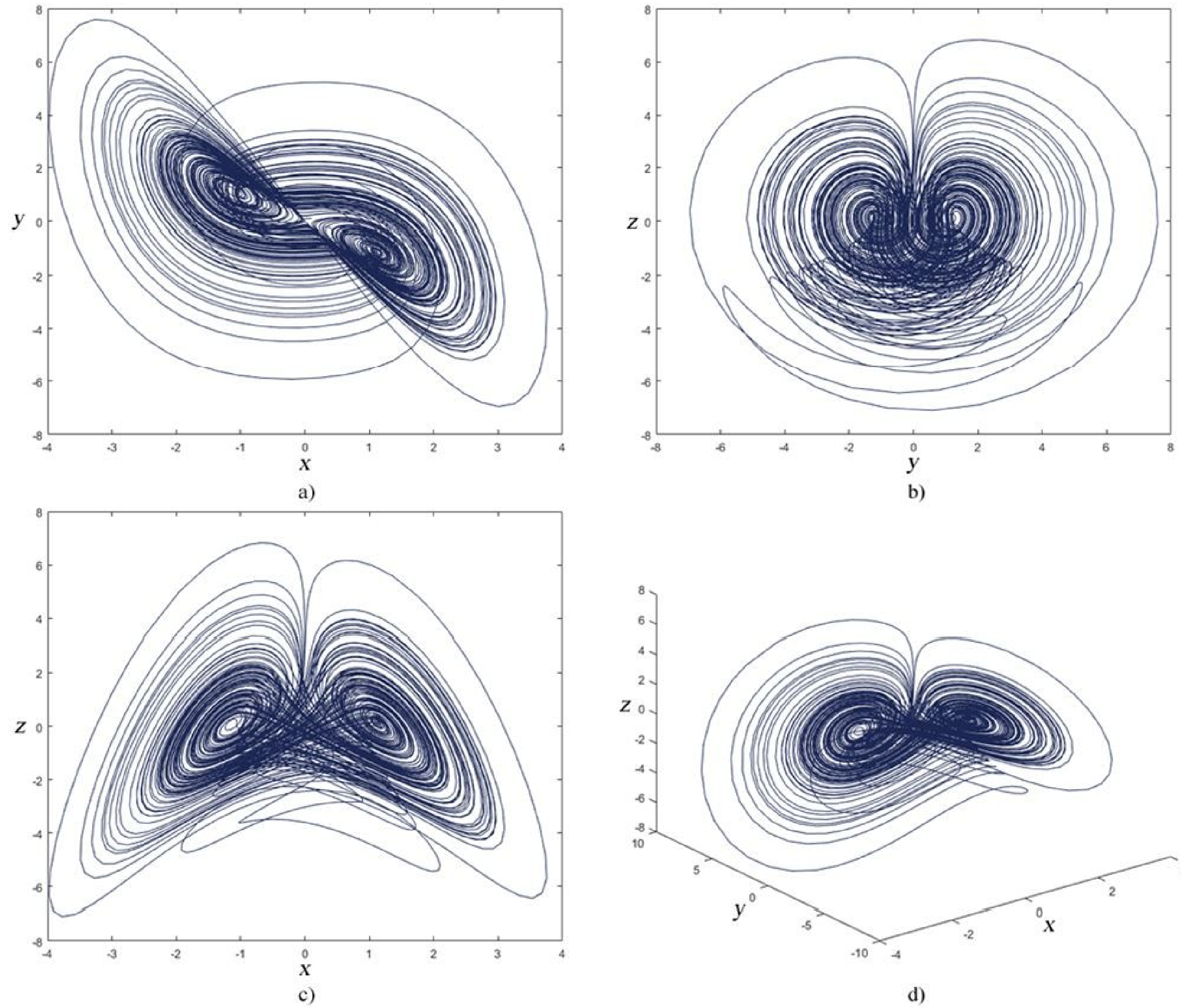

Figure 3

Phase portraits of a Burke-Shaw chaotic attractor: a) x-y, b) y-z, c) x-z, d) x-y-z.

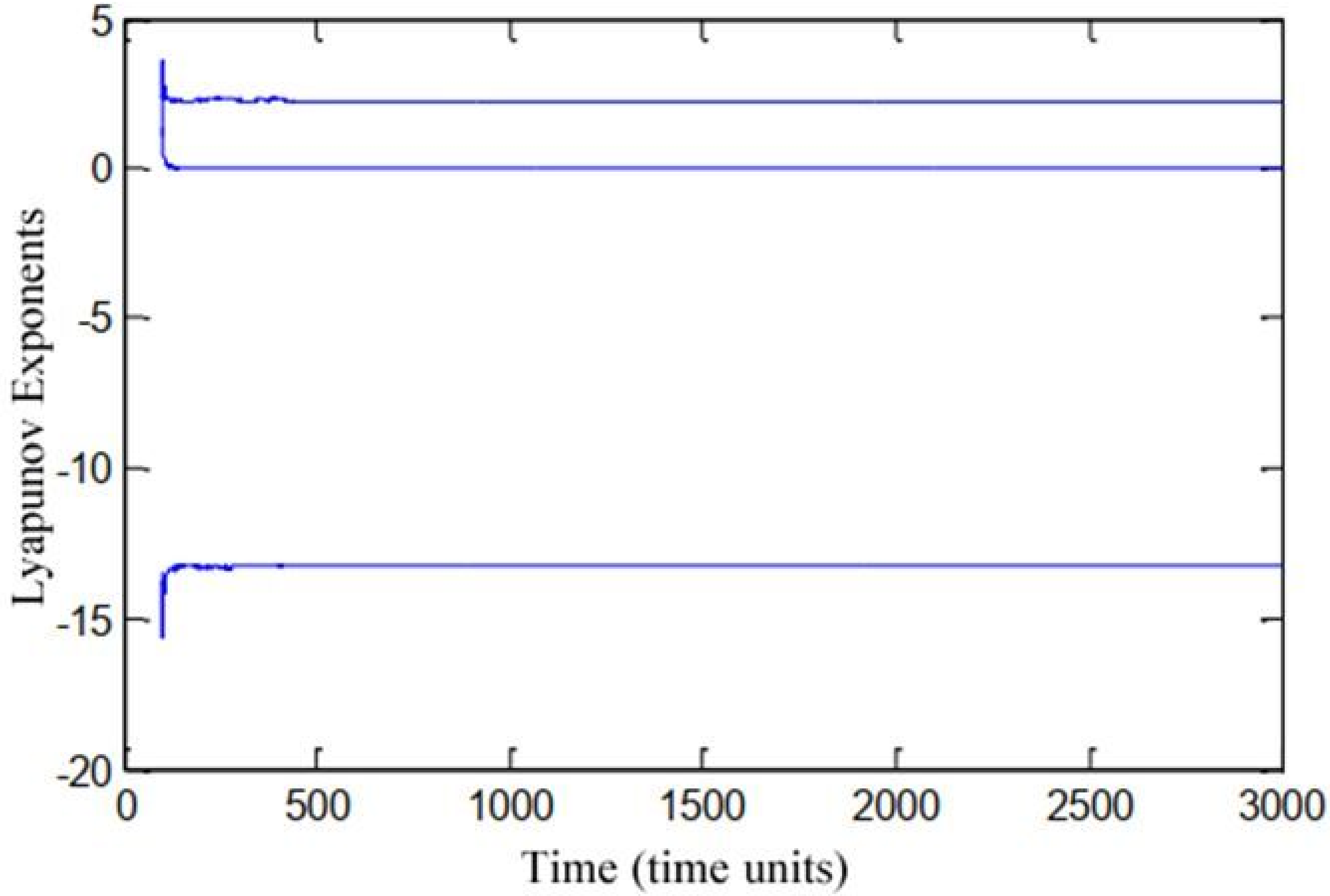

Figure 4

Lyapunov exponents of a Burke-Shaw chaotic attractor.

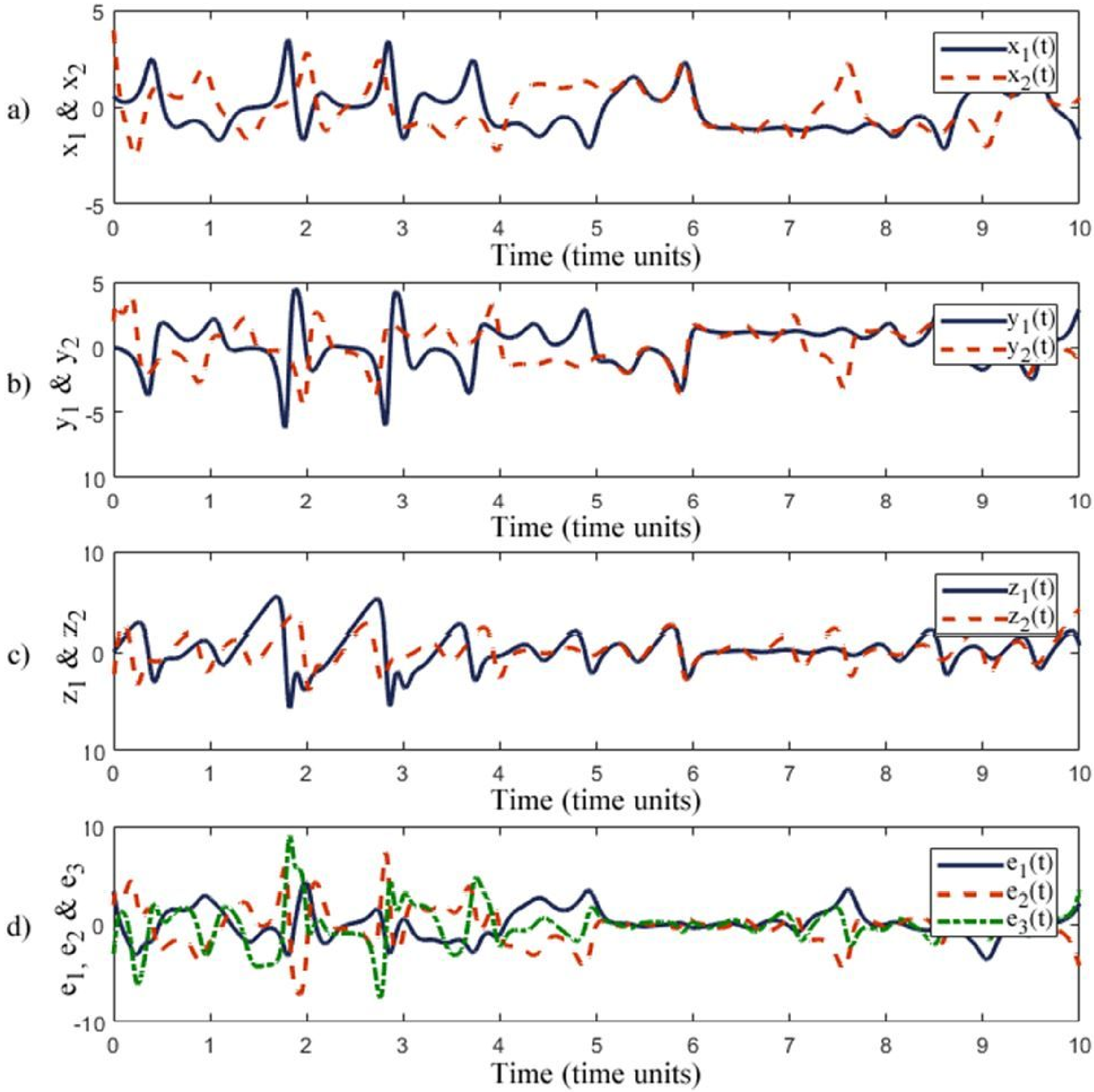

Figure 5

Before active control synchronization (a) driving and response signal (x1, x2), (b) y1 and y2 , (c) z1 and z2, (d) errors (e1 = x1-x2, e2 = y1-y2, e3 = z1-z2)

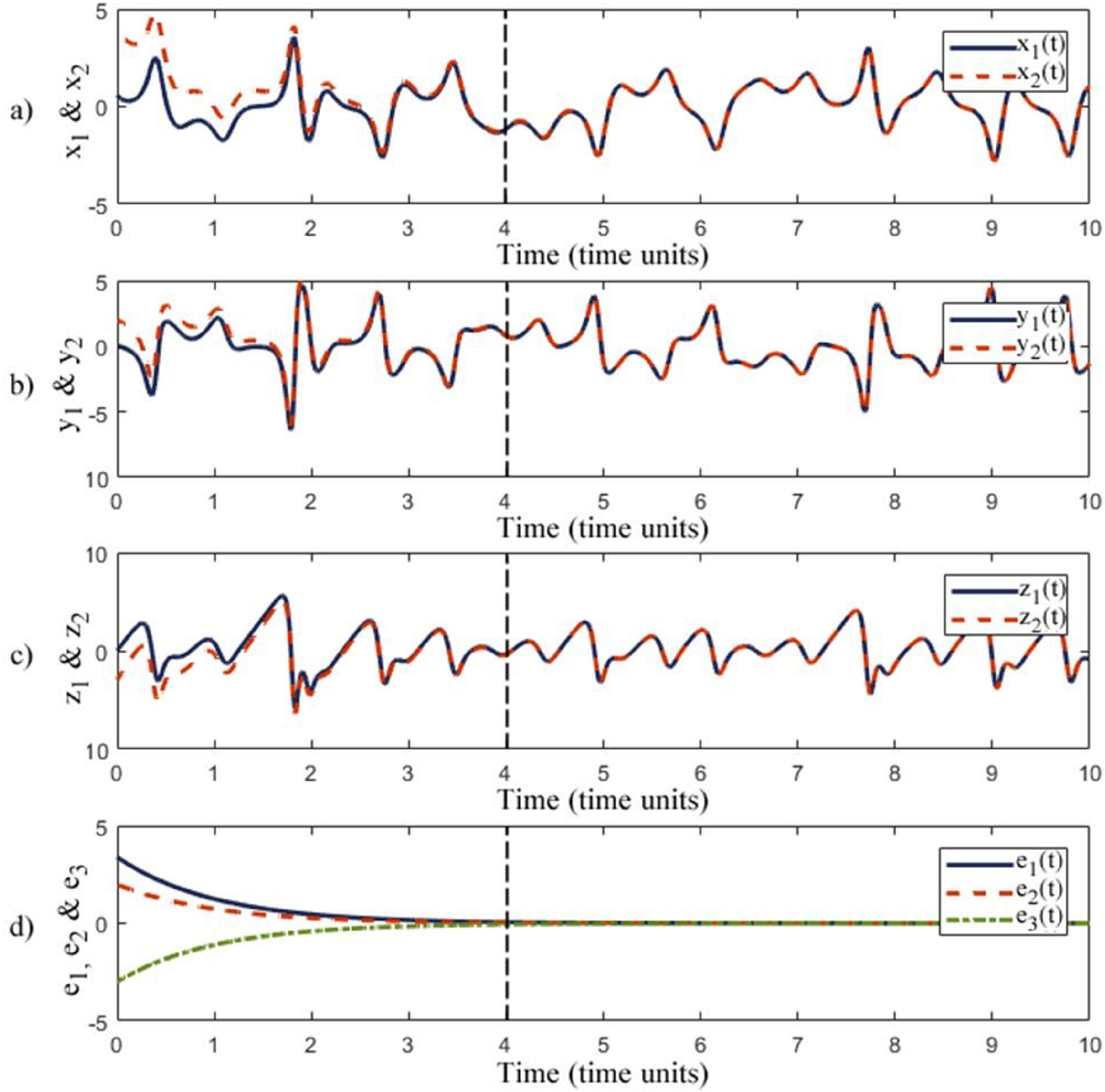

Figure 6

Post active control synchronization (a) driving and response signal (x1, x2), (b) y1 and y2 , (c) z1 and z2, (d) errors (e1 = x1-x2, e2 = y1-y2, e3 = z1-z2)

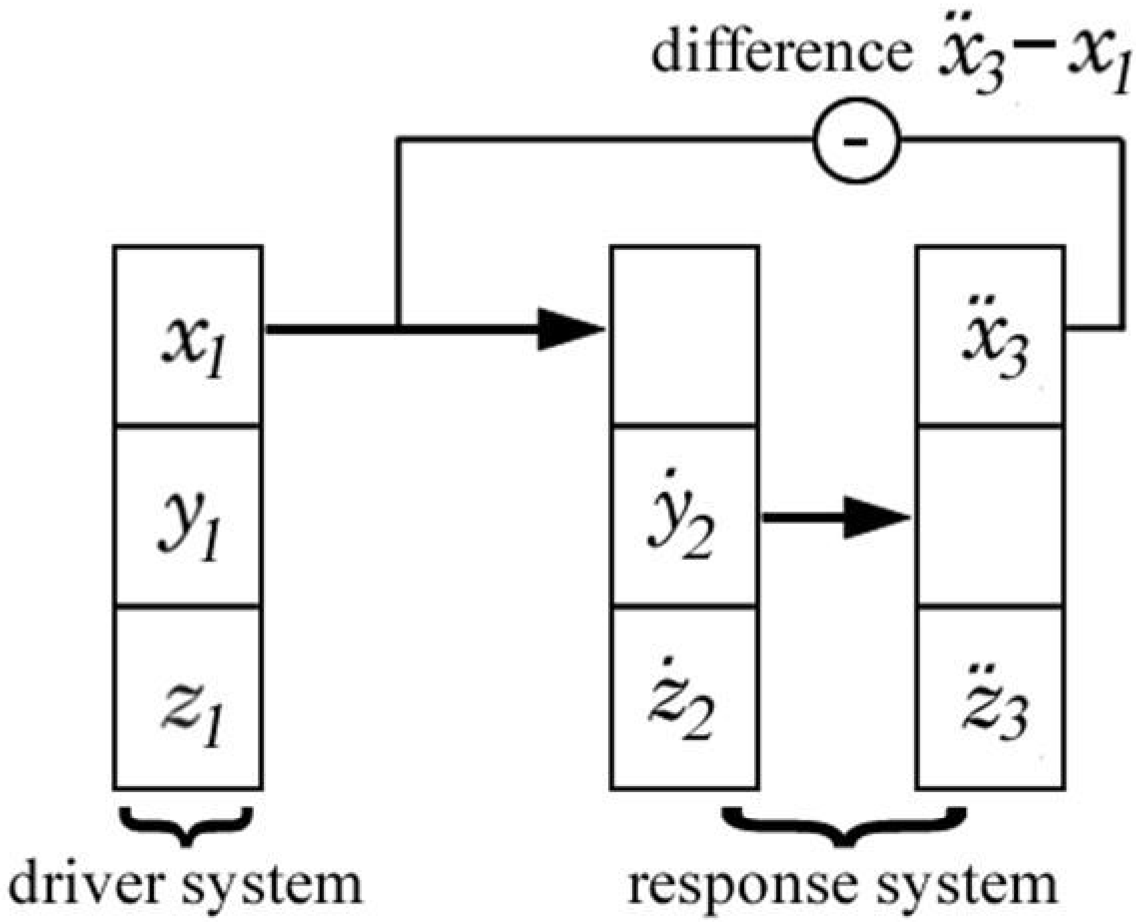

Figure 7

The block diagram of P-C synchronization [1].

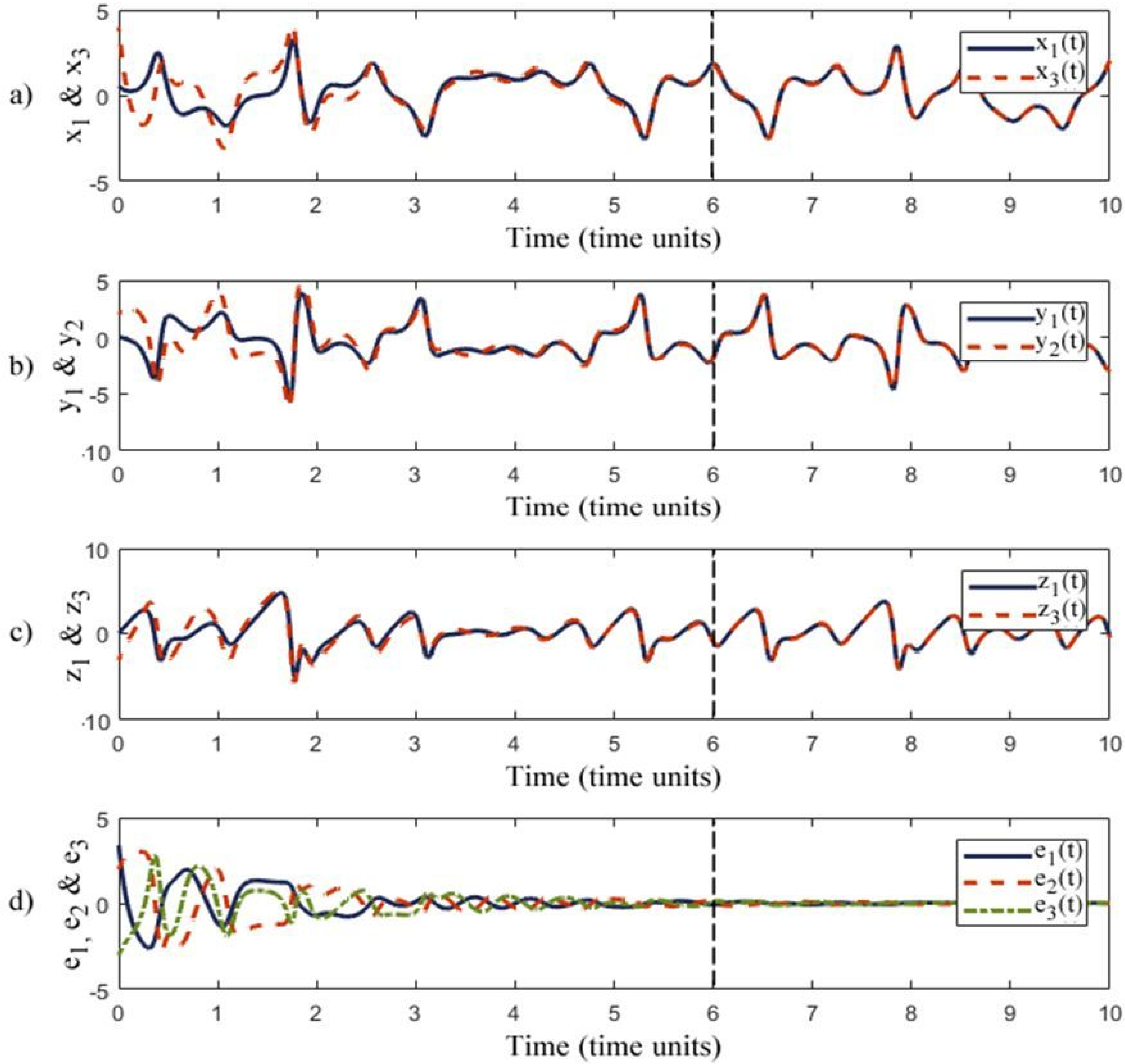

Figure 8

Post P-C synchronization with integer-order (a) driving and response signal (x1, x3), (b) y1 and y2 , (c) z1 and z3, (d) errors (e1 = x1-x3, e2 = y1-y2, e3 = z1-z3)

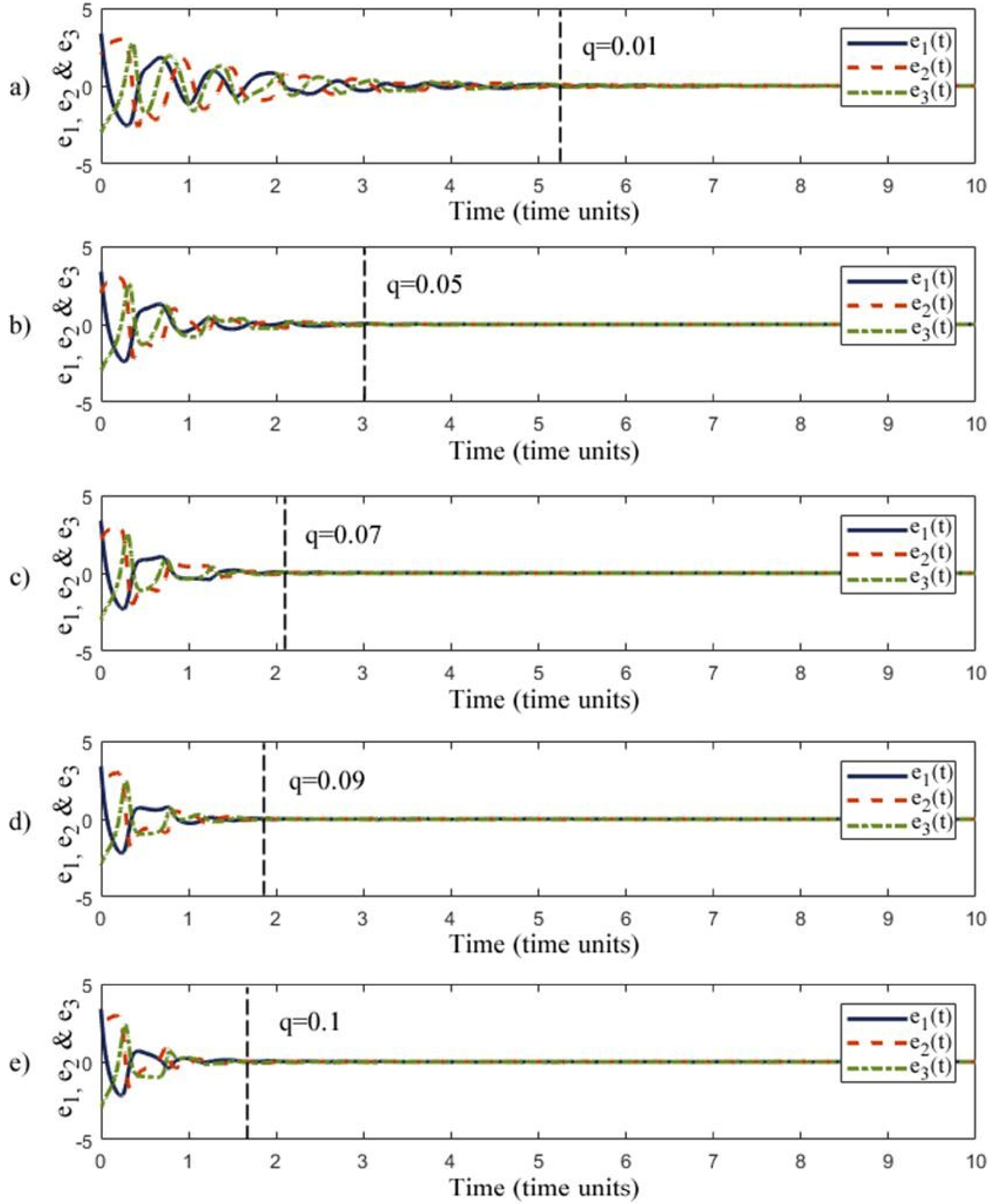

Figure 9

Post P-C synchronization with fractional-order errors for various fractional-order q values

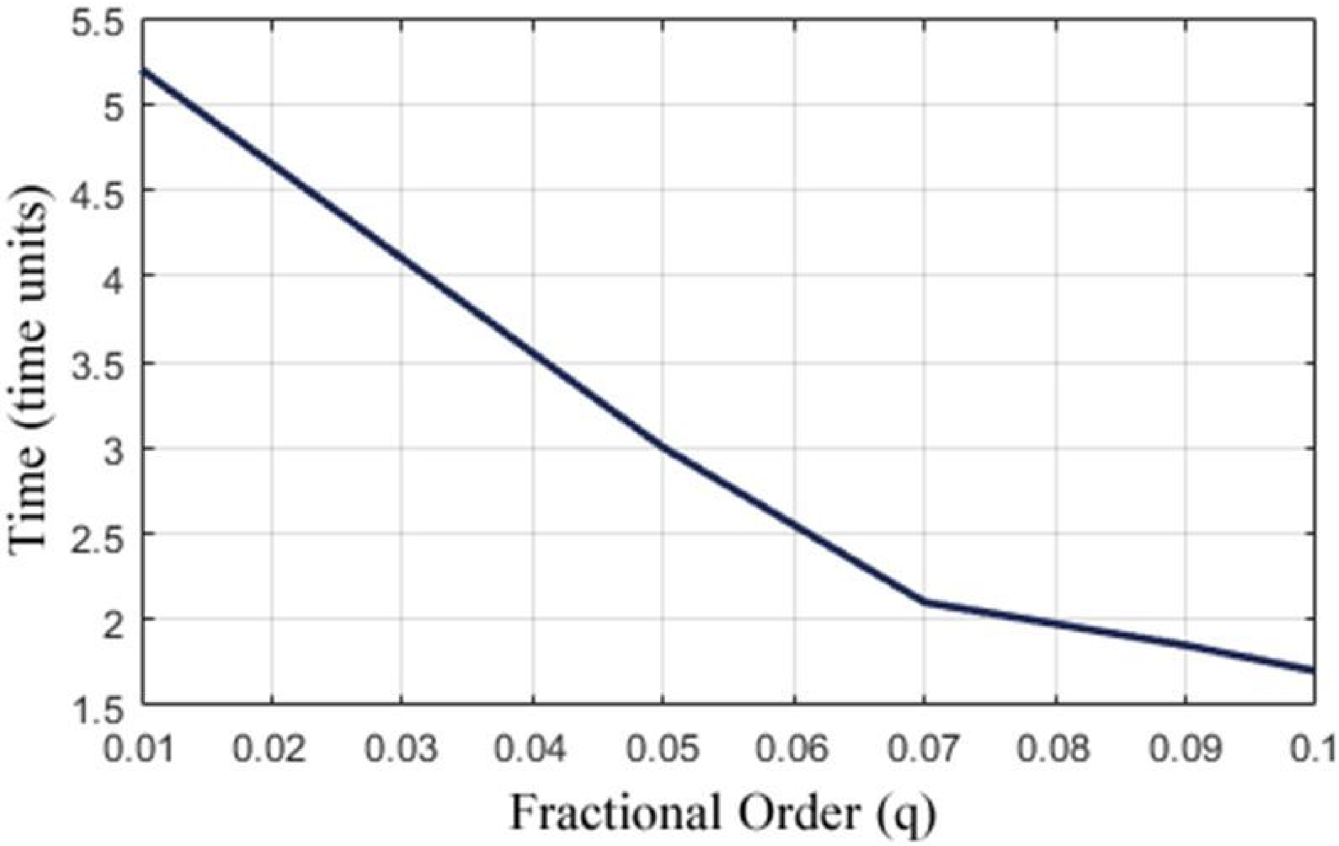

Figure 10

Post P-C synchronization with fractional-order times for various fractional-order q values